Int. J. Heat Mass Transfer. Vol. 31, No. 12, pp. 2579–2585, 1988
Printed in Great Britain

0017-9310/88 $3.00+0.00

Parameter estimation for packed cooling tower operation using a heat input-response technique

S. KAGUEI, M. NISHIO and N. WAKAO†
Faculty of Engineering, Yokohama National University, Yokohama 240, Japan

(*Received* 25 *January* 1988 *and in final form* 19 *April* 1988)

Abstract—A method is proposed for predicting the variations of air and water temperatures and of air humidity in a packed bed counterflow type of cooling tower subjected to a thermal disturbance. Heat input-response measurements are carried out by imposing thermal disturbances on inlet water and inlet air. The air-film and water-film heat transfer coefficients are estimated by fitting in the time domain the measured output temperature/humidity variations to those predicted.

INTRODUCTION

A LOT OF work has been conducted on the heat input-response measurements in two-phase (solid and gas) packed beds (see, e.g. refs. [1–4]), while less attention has been focused on the dynamic thermal behavior of three-phase (solid, gas and liquid) packed beds. Most investigations on cooling towers have been made under steady-state conditions [5–11]. Recently, Younis *et al.* [12] carried out heat input-response measurements in a packed bed type of cooling tower, and obtained the relationships between the air-side and water-side heat transfer coefficients.

THEORETICAL

The system considered is a packed bed type of countercurrently operated cooling tower subjected to one-shot thermal disturbances in the inlet water and/or inlet air. The theoretical treatment is based on the following assumptions.

(1) The column is adiabatic.

(2) As packing, solid cylinders are horizontally placed loosely in the tower. These simulate the actual use of wire netting. The cylinder surface is completely wetted by water.

(3) No temperature gradient exists across the water film covering the solid packing.

(4) The parameters involved in the heat and mass transfer process remain unchanged in the tower.

(5) The saturation humidity is expressed approximately as a linear function of temperature.

The air temperature (T_G), water temperature (T_L), solid temperature (T_P), air humidity (Y), temperature at the air–water interface (T_i) and the saturation humidity (Y_i) are expressed, respectively, as

$$T_G = T_G^\infty + T'_G \quad (1)$$

$$T_L = T_L^\infty + T'_L \quad (2)$$

$$T_P = T_P^\infty + T'_P \quad (3)$$

$$Y = Y^\infty + Y' \quad (4)$$

$$T_i = T_i^\infty + T'_i \quad (5)$$

$$Y_i = Y_i^\infty + Y'_i \quad (6)$$

where the first terms on the right-hand side with superscript ∞ show the steady state, and the second terms correspond to the variations due to the thermal disturbance. The variations are then expressed as [12]

for the air phase

$$\varepsilon_G \rho_G C_G \frac{\partial T'_G}{\partial t} = -G C_G \frac{\partial T'_G}{\partial x} - h_G a (T'_G - T'_i) \quad (7)$$

$$\varepsilon_G \rho_G \frac{\partial Y'}{\partial t} = -G \frac{\partial Y'}{\partial x} + k_y a (Y'_i - Y'); \quad (8)$$

for the water phase

$$\varepsilon_L \rho_L C_L \frac{\partial T'_L}{\partial t} = L C_L \frac{\partial T'_L}{\partial x} - h_L a (T'_L - T'_i) - h_P a_p \{T'_L - (T'_P)_R\}; \quad (9)$$

at the air–water interface

$$h_G a (T'_G - T'_i) + h_L a (T'_L - T'_i) = k_y a \lambda (Y'_i - Y'); \quad (10)$$

for the solid phase

$$\frac{\partial T'_P}{\partial t} = \alpha_P \frac{1}{r} \frac{\partial}{\partial r}\left(r \frac{\partial T'_P}{\partial r}\right); \quad (11)$$

† Author to whom correspondence should be addressed.

NOMENCLATURE

a	air–water contact area per unit volume of tower [m^{-1}]
a_P	surface area of solid packing per unit volume of tower [m^{-1}]
B	temperature effect on saturation humidity [K^{-1}]
C_G	specific heat of air [$J\,kg^{-1}\,K^{-1}$]
C_L	specific heat of water [$J\,kg^{-1}\,K^{-1}$]
G	mass velocity of air [$kg\,m^{-2}\,s^{-1}$]
h_G	heat transfer coefficient for air at the air–water interface [$W\,m^{-2}\,K^{-1}$]
h_L	heat transfer coefficient for water at the air–water interface [$W\,m^{-2}\,K^{-1}$]
h_P	heat transfer coefficient for water at the solid packing surface [$W\,m^{-2}\,K^{-1}$]
J_0, J_1	Bessel functions of the first kind and of zeroth and first orders, respectively
k_P	thermal conductivity of wire [$W\,m^{-1}\,K^{-1}$]
k_y	mass transfer coefficient for water vapor at the air–water interface [$kg\,m^{-2}\,s^{-1}$]
L	mass velocity of water [$kg\,m^{-2}\,s^{-1}$]
R	radius of wire [m]
r	radial distance variable [m]
s	Laplace operator [s^{-1}]
T_G	air temperature [K]
T_i	temperature at the air–water interface [K]
T_L	water temperature [K]
T_P	solid temperature [K]
t	time [s]
X	height of packed tower [m]
x	axial distance variable [m]
Y	air humidity [kg (water) kg^{-1} (dry air)]
Y_i	saturation humidity [kg (water) kg^{-1} (dry air)].

Greek symbols

α_P	thermal diffusivity of solid packing [$m^2\,s^{-1}$]
ε	r.m.s. error between measured and predicted output variations
ε_G	air volume fraction
ε_L	water volume fraction
ε_P	volume fraction of wire in tower
λ	latent heat of vaporization of water [$J\,kg^{-1}$]
ρ_G	density of air [$kg\,m^{-3}$]
ρ_L	density of water [$kg\,m^{-3}$].

Superscripts

I	tower bottom
II	tower top
∞	steady state
$'$	variations.

at the solid surface

$$k_P \frac{\partial T_P'}{\partial r} = h_P(T_L' - T_P') \quad \text{at } r = R. \tag{12}$$

The initial conditions are given by

$$T_G' = T_L' = T_P' = T_i' = Y' = Y_i' = 0 \quad \text{at } t = 0. \tag{13}$$

Using the Lewis relation

$$\frac{h_G}{k_y} = C_G \tag{14}$$

and the following approximation:

$$Y_i = A + BT_i \tag{15}$$

or

$$Y_i' = BT_i' \tag{15a}$$

together with the initial conditions the basic equations are Laplace transformed. Note that $\bar{T}_G$, $\bar{Y}$ and $\bar{T}_L$ are, respectively, the transforms of T_G', Y' and T_L'. For example

$$\bar{T}_G = \int_0^\infty T_G' \exp(-st)\,dt. \tag{16}$$

We then obtain

$$\begin{bmatrix} (\bar{T}_G)^{II} \\ (\bar{Y})^{II} \\ (\bar{T}_L)^{II} \end{bmatrix} = [F] \begin{bmatrix} (\bar{T}_G)^{I} \\ (\bar{Y})^{I} \\ (\bar{T}_L)^{I} \end{bmatrix} \tag{17}$$

where superscripts I and II, respectively, represent the tower bottom and the tower top. The transfer matrix $[F]$ is given by

$$[F] = \sum_{k=1}^{3} [M_k] \exp\{(p_k - Cs)X\} \tag{18}$$

$$[M_1] = \frac{1}{1-\gamma} \begin{bmatrix} \beta B & -\beta & 0 \\ -\alpha B & \alpha & 0 \\ 0 & 0 & 0 \end{bmatrix} \tag{18a}$$

$$[M_2] = \frac{H_G}{p_2 - p_3} [M(p_2)] \tag{18b}$$

$$[M_3] = \frac{H_G}{p_3 - p_2} [M(p_3)] \tag{18c}$$

$$[M(p)] = \begin{bmatrix} \alpha q & \beta q & \gamma \\ \alpha B q & \beta B q & \gamma B \\ -\dfrac{\alpha H_L}{H_G} & -\dfrac{\beta H_L}{H_G} & \dfrac{p + \gamma H_G}{H_G} \end{bmatrix} \tag{18d}$$

$$C = \frac{\varepsilon_G \rho_G}{G} \tag{18e}$$

$$D = \left(\frac{\varepsilon_G \rho_G}{G} + \frac{\varepsilon_L \rho_L}{L}\right)s + \frac{k_P a_P}{LC_L R} \frac{1}{\dfrac{k_P}{h_P R} - \dfrac{J_0(\phi)}{\phi J_1(\phi)}} \tag{18f}$$

$$H = \gamma H_G - (1-\gamma)H_L \tag{18g}$$

$$H_G = \frac{h_G a}{GC_G} \tag{18h}$$

$$H_L = \frac{h_L a}{LC_L} \tag{18i}$$

$$p_1 = -H_G \tag{18j}$$

$$p_2, p_3 = \frac{H-D}{2}\left\{-1 \pm \sqrt{\left(1 + \frac{4DH_G\gamma}{(H-D)^2}\right)}\right\} \tag{18k}$$

$$q = \frac{p - H_L - D}{p + H_G} \tag{18l}$$

$$\alpha = \frac{h_G a}{\psi} \tag{18m}$$

$$\beta = \frac{h_G a \lambda}{C_G \psi} \tag{18n}$$

$$\gamma = \frac{h_L a}{\psi} \tag{18o}$$

$$\phi = R\sqrt{\left(-\frac{s}{\alpha_P}\right)} \tag{18p}$$

$$\psi = h_G a\left(1 + \frac{\lambda B}{C_G}\right) + h_L a. \tag{18q}$$

Therefore, once the input disturbances, $(T'_G)^{I}$ and/or $(Y')^{I}$ and/or $(T'_L)^{II}$, are measured with time, the output variations, $(T'_G)^{II}$, $(Y')^{II}$ and $(T'_L)^{I}$, may be predicted as functions of time. These calculations may be performed by expanding the input signals and the transfer functions as Fourier series [13].

Also, we find from equations (7), (8), (14) and (15a) that

$$\varepsilon_G \rho_G C_G \frac{\partial Z}{\partial t} = -GC_G \frac{\partial Z}{\partial x} - h_G a Z \tag{19}$$

where

$$Z = T'_G - \frac{Y'}{B}. \tag{19a}$$

Therefore

$$(Z(t))^{II} = \exp(-H_G X)(Z(t-CX))^{I}. \tag{20}$$

It is interesting to note that $(T'_G)^{II} - (Y')^{II}/B$ is a function only of $h_G a$, although $(T'_G)^{II}$ and $(Y')^{II}$ are functions of $h_G a$ and $h_L a$.

Disturbance on inlet water

When the thermal disturbance is given in terms of the change in inlet water temperature, while the temperature and humidity of the inlet air remain unchanged, i.e. $(T'_G)^{I} = (Y')^{I} = 0$ and then $(\bar{T}_G)^{I} = (\bar{Y})^{I} = 0$, equation (17) reduces to

$$(\bar{T}_G)^{II} = \frac{F_{13}}{F_{33}}(\bar{T}_L)^{II} \tag{21}$$

$$(\bar{Y})^{II} = \frac{F_{23}}{F_{33}}(\bar{T}_L)^{II} \tag{22}$$

$$(\bar{T}_L)^{I} = \frac{1}{F_{33}}(\bar{T}_L)^{II} \tag{23}$$

where F_{ij} is the (i,j)th element of transfer matrix $[F]$. The matrix elements, F_{13}, F_{23} and F_{33}, are explicitly expressed as

$$F_{13} = \frac{H_G\gamma}{p_2 - p_3}[1 - \exp\{(p_3 - p_2)X\}] \times \exp\{(p_2 - Cs)X\} \tag{23a}$$

$$F_{23} = BF_{13} \tag{23b}$$

$$F_{33} = \frac{p_2 + \gamma H_G}{p_2 - p_3}\left[1 - \frac{p_3 + \gamma H_G}{p_2 + \gamma H_G}\exp\{(p_3 - p_2)X\}\right] \times \exp\{(p_2 - Cs)X\}. \tag{23c}$$

Therefore, for a cooling tower subjected to the thermal disturbance of inlet water, equations (21), (22) and (23b) indicate that $(\bar{Y})^{II}$ is equal to $B(\bar{T}_G)^{II}$. It also indicates that if one of the three signals, $(T'_L)^{I}$, $(T'_L)^{II}$ and $(T'_G)^{II}$ (or $(Y')^{II}$), is measured with time, the other two may be predicted.

Disturbance on inlet air

When a thermal disturbance is given by the change in inlet air temperature, $(Y')^{I} = (T'_L)^{II} = 0$, and equation (17) reduces to

$$(\bar{T}_G)^{II} = \left(F_{11} - \frac{F_{13}F_{31}}{F_{33}}\right)(\bar{T}_G)^{I} \tag{24}$$

$$(\bar{Y})^{II} = \left(F_{21} - \frac{F_{23}F_{31}}{F_{33}}\right)(\bar{T}_G)^{I} \tag{25}$$

$$(\bar{T}_L)^{I} = -\frac{F_{31}}{F_{33}}(\bar{T}_G)^{I}. \tag{26}$$

Therefore, if one of the four signals, $(T'_G)^{I}$, $(T'_L)^{I}$, $(T'_G)^{II}$ and $(Y')^{II}$, is measured with time, the other three may be predicted.

EXPERIMENTAL

The apparatus employed was identical with that of Younis *et al.* [12]. The tower made of polystyrene foam was packed with corrugated stainless steel wire netting of diameter 0.4 mm. Air was introduced to the bottom of the tower and water to the top. The air and water temperatures at either end of the tower were

Table 1. Experimental conditions and steady-state data

	Run No. 1	Run No. 2
Tower, cylindrical:		
inside diameter, m	0.075	0.075
height, m	0.05	0.05
Mass velocity of air, kg m^{-2} s^{-1}	0.26	0.26
Mass velocity of water, kg m^{-2} s^{-1}	0.38	0.39
At the tower top:		
water temperature, °C	20.7	20.6
air temperature, °C	16.0	15.8
air humidity, kg (water) kg^{-1} (dry air)	0.0094	0.0090
At the tower bottom:		
water temperature, °C	17.1	17.1
air temperature, °C	16.5	16.1
air humidity, kg (water) kg^{-1} (dry air)	0.0006	0.0007

Run Nos. 1 and 2: steady-state operations before cold water was imposed at the tower top and warm air was introduced to the tower bottom, respectively.

measured by thermistors. The humidities of inlet air and outlet air were measured by humidity-measuring elements (Shibaura Electronic Co., Tokyo, Model CHS-1-H1). Preliminary experiments with the empty column, where water falls like rain, subjected to a one-shot thermal pulse on the inlet water, showed that the peak humidity of the outlet air measured by the element always appeared 30 s behind that of the air temperature measured by the thermistor. Therefore, all the humidity–time curves shown in this paper have been adjusted for the time lag by shifting the time scale 30 s earlier. The experimental conditions and steady-state data are listed in Table 1.

Figures 1(a) and (b) show the temperatures of water and the temperatures and humidities of air measured at either end of the tower, respectively, when the inlet water at the top of the tower was switched to colder water for a limited period of time and when the inlet air was heated for a limited time before entering the bottom of the tower.

PREDICTION OF RESPONSE TEMPERATURES

Disturbance on inlet water

Using the input data of $(T'_L)^{II}_{exptl}$ recorded with time and the parameter values listed in Table 2, the response temperatures, $(T'_L)^I$ and $(T'_G)^{II}$, are predicted from equations (23) and (21), respectively, as shown in Fig. 2(a).

Disturbance on inlet air

Similar calculations for $(T'_G)^{II}$ and $(T'_L)^I$ are performed, respectively, from equations (24) and (26) with the input data of $(T'_G)^{II}_{exptl}$ and the parameter values of Table 2, with the results shown in Fig. 2(b).

As depicted in Figs. 2(a) and (b), the response temperatures predicted are in good agreement with those measured. In these calculations, $h_P a_P$ was temporarily assumed to be 10000 W m^{-3} K^{-1} and ε_L was 0.01. However, it was found that $h_P a_P$ and ε_L had little effect on the prediction of temperature response curves. Any $h_P a_P$ value in the range 1 to ∞ and any ε_L value less than 0.1 caused no appreciable difference in the

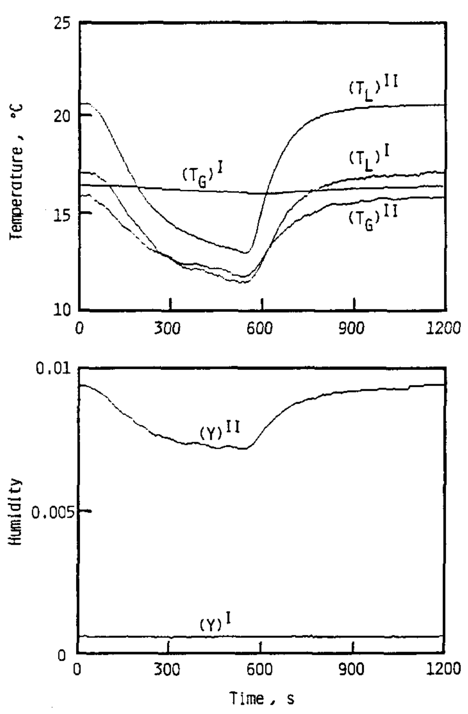

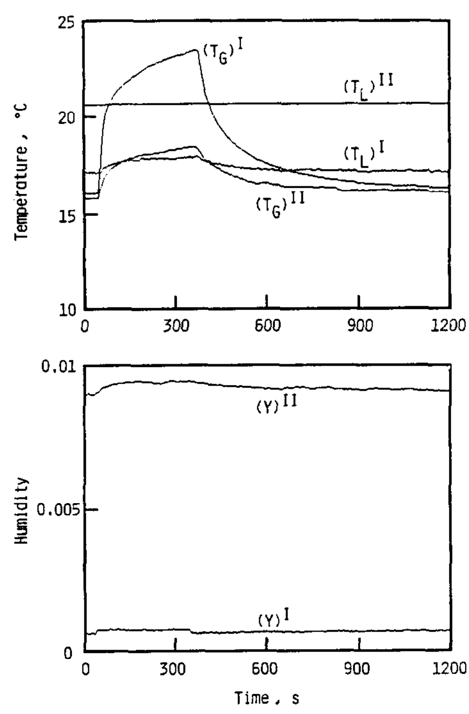

FIG. 1. Temperatures and humidities measured at either end of the tower: (a) cold water introduced to the tower top; (b) warm air introduced to the tower bottom.

Table 2. Data used for the prediction of temperature and humidity variations

Height of tower	$X = 0.05$ m
Air:	
mass velocity	$G = 0.26$ kg m^{-2} s^{-1}
density	$\rho_G = 1.21$ kg m^{-3}
specific heat	$C_G = 1.02$ kJ kg^{-1} K^{-1}
volume fraction	$\varepsilon_G = 1-\varepsilon_L-\varepsilon_P$
Water:	
mass velocity	$L = 0.38$ kg m^{-2} s^{-1}
density	$\rho_L = 1000$ kg m^{-3}
specific heat	$C_L = 4.18$ kJ kg^{-1} K^{-1}
volume fraction	$\varepsilon_L = 0.01$†
Stainless steel wire netting:	
radius of wire	$R = 0.2$ mm
thermal conductivity	$k_P = 19$ W m^{-1} K^{-1}
thermal diffusivity	$\alpha_P = 5.3 \times 10^{-6}$ m^2 s^{-1}
volume fraction	$\varepsilon_P = 0.015$
Latent heat of vaporization	$\lambda = 2460$ kJ kg^{-1}
Temperature effect on saturation humidity	$B = 0.0008$ K^{-1}‡
Heat transfer coefficients	$h_G a = 8000$ W m^{-3} K^{-1}‡
	$h_L a = 30\,000$ W m^{-3} K^{-1}‡
	$h_P a_P = 10\,000$ W m^{-3} K^{-1}†

† Assumed.
‡ Estimated from steady-state operations.

response curves obtained. Some difference resulted when ε_L was larger than 0.1, a value which is, however, unrealistically large.

PARAMETER ESTIMATION BY CURVE-FITTING IN THE TIME DOMAIN

The values of the three parameters, B, $h_G a$ and $h_L a$, employed for predicting the temperature responses in the preceding section were obtained from steady-state operations. Determination of the values of these three parameters under dynamic conditions is studied in this section.

Disturbance on inlet water

Using the experimentally measured $(T_L')^{II}_{exptl}$–t curve and various assumed values of B, $h_G a$ and $h_L a$, $(T_L')^{I}$–t and $(T_G')^{II}$–t curves are predicted from equations (23) and (21), respectively. Figure 3(a) is an error map indicating the effects of B and $h_L a$ on the calculations of $(T_L')^{I}$–t and $(T_G')^{II}$–t curves, when $h_G a$ is fixed at 8000 and 10^6 W m^{-3} K^{-1}. The solid-line contours for $(T_L')^{I}$, for instance, indicate that the B and $h_L a$ values within the two contours, using a $h_G a$ value of 8000 W m^{-3} K^{-1}, give the predicted $(T_L')^{I}$–t curves different from the measured curve, $(T_L')^{I}_{exptl}$–t, by less than the r.m.s. error of 10%. A similar error map showing the effects of B and $h_G a$ at selected $h_L a$ values of 30 000 and 10^6 W m^{-3} K^{-1} is illustrated in Fig. 3(b).

In Fig. 3(a) for the case where $h_G a$ is 8000 W m^{-3} K^{-1}, the values of B and $h_L a$ may be determined from the hatched area where the pair of solid-line contour planes overlap. When $h_G a$ is 10^6 W m^{-3} K^{-1}, another set of B and $h_L a$ are obtained from the hatched area where the two dotted-line contour planes overlap. Also, from the hatched areas in Fig. 3(b) two sets of B and $h_G a$ values are obtained corresponding to the two $h_L a$ values of 30 000 and 10^6 W m^{-3} K^{-1}. The values of $h_L a$ (or $h_G a$) thus obtained are found to depend upon the assumed values of $h_G a$ (or $h_L a$).

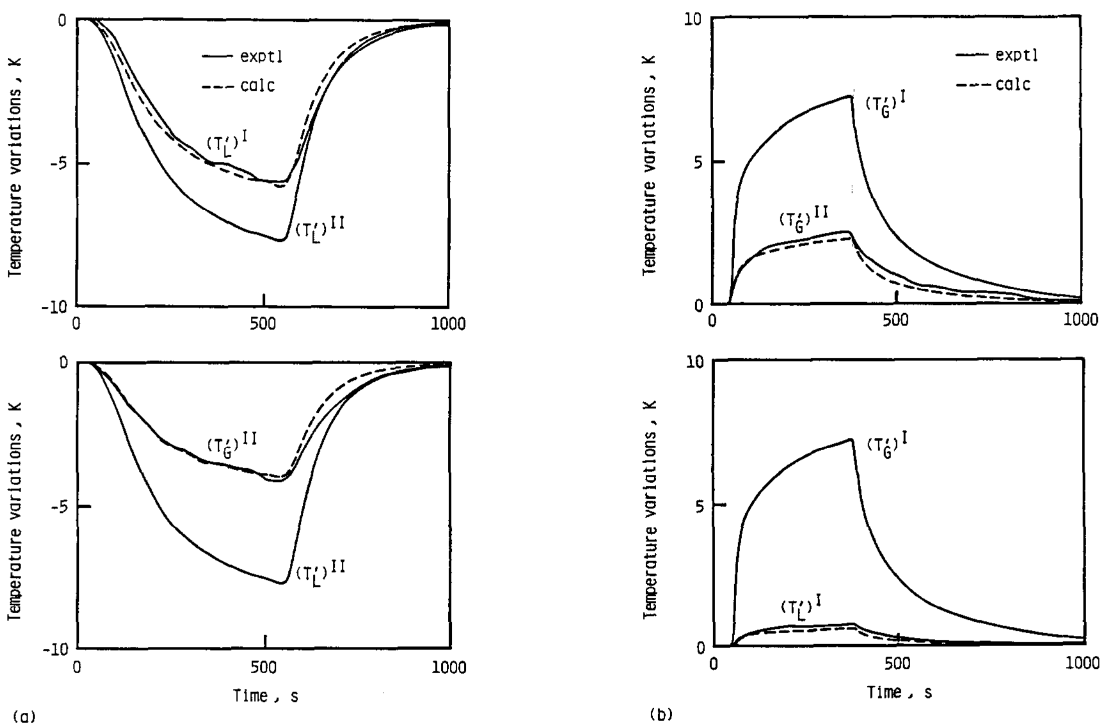

FIG. 2. Comparison between measured temperature variations and those predicted: (a) cold water introduced to the tower top; (b) warm air introduced to the tower bottom.

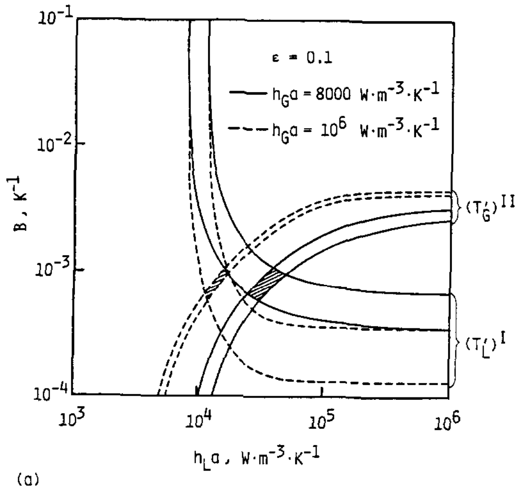

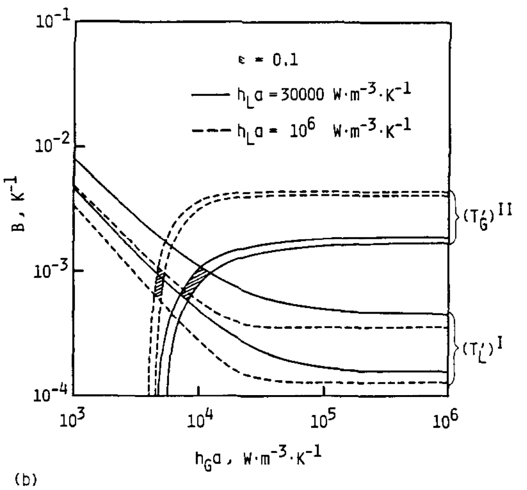

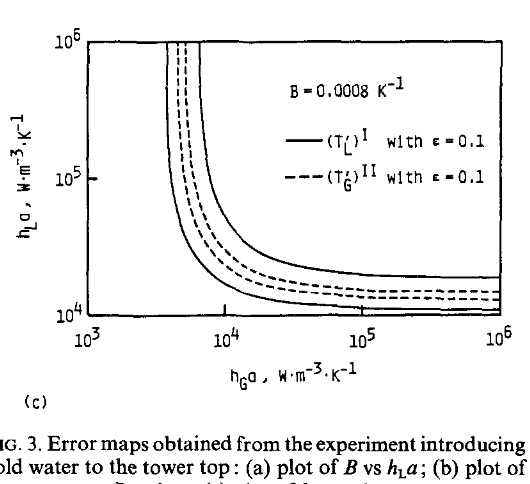

FIG. 3. Error maps obtained from the experiment introducing cold water to the tower top: (a) plot of B vs h_La; (b) plot of B vs h_Ga; (c) plot of h_La vs h_Ga.

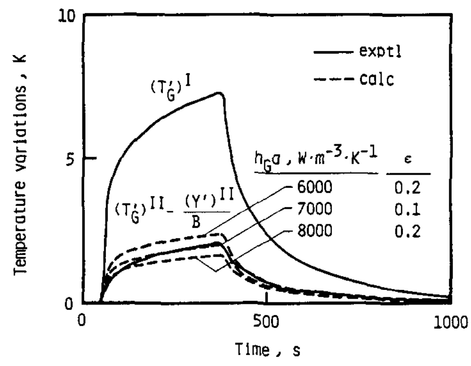

FIG. 4. Comparison between measured $(T'_G)^{II} - (Y')^{II}/B$ and those predicted.

However, the value of B is almost independent of the h_La and h_Ga values: from Figs. 3(a) and (b) the value of B is found to be in the narrow range from 0.0006 to 0.0010 K^{-1} or roughly 0.0008 K^{-1}.

Using this B value thus determined, h_La–h_Ga relationships are calculated as shown in Fig. 3(c). The contour planes for $(T'_L)^I$ and $(T'_G)^{II}$ again indicate, respectively, that the $(T'_L)^I$ and $(T'_G)^{II}$ curves predicted with the h_La and h_Ga values within the contours agree with the corresponding measured response curves within the r.m.s. error of 10%. The contour plane for $(T'_L)^I$ with the r.m.s. error of 0.1 is wider than that for $(T'_G)^{II}$ with $\varepsilon = 0.1$, but the two contour planes are of the same hyperbolic type and the latter lies within the former. Similar h_La–h_Ga relationships of hyperbolic type were obtained by Younis *et al.* [12], from experiments based on the thermal disturbance of the inlet water.

Disturbance on inlet air

Using the B value already determined and $(T'_G)^{II}_{exptl}$–t and $(Y')^{II}_{exptl}$–t curves, $(T'_G)^{II}_{exptl} - (Y')^{II}_{exptl}/B$ values are obtained as a function of time, as shown together with the $(T'_G)^{I}_{exptl}$–t curve in Fig. 4.

The function, $\{(T'_G)^{II} - (Y')^{II}/B\}_{calc}$, can be computed from equation (20). In the computations h_Ga were assumed to be 6000, 7000 and 8000 W m^{-3} K^{-1}. As shown in Fig. 4, the curve predicted with $h_Ga = 7000$ W m^{-3} K^{-1} agrees reasonably well with the measured curve (r.m.s. error of 10%).

Using this h_Ga value, h_La is estimated from the contour for $(T'_G)^{II}$ with $\varepsilon = 0.1$ in Fig. 3(c) to be from 40 000 to 50 000 W m^{-3} K^{-1} or roughly 45 000 W m^{-3} K^{-1}. It should be noted that the values determined from the dynamic operations seem reasonable in comparison to those ($B = 0.0008$ K^{-1}, $h_Ga = 8000$ and $h_La = 30\,000$ W m^{-3} K^{-1}, as listed in Table 2) obtained from the steady-state operations.

CONCLUSIONS

Two dynamic experiments were carried out in a countercurrent type cooling tower at almost the same air and water flow rates: a thermal disturbance given to the inlet water and one imposed on the inlet air. The temperature of the outlet water and the temperature and humidity of the outlet air predicted were in good agreement with those measured. The experiment imposing the thermal disturbance on the inlet water determined the value of B (which gives the temperature effect on saturation humidity) and a relationship between $h_L a$ and $h_G a$. These were obtained by curve-fitting in the time domain of the measured outlet temperatures of air and water to those predicted.

From the experiment giving the thermal disturbance on the inlet air, $h_G a$ was determined by time domain fitting of the $(T'_G)^{II}_{exptl} - (Y')^{II}_{exptl}/B$ curve. Consequently, $h_L a$ was also determined. These $h_G a$ and $h_L a$ values thus determined from the dynamic operations were found to agree reasonably with those obtained from the steady-state operations.

REFERENCES

1. H. Littman, R. G. Barile and A. H. Pulsifer, Gas–particle heat transfer coefficients in packed beds at low Reynolds numbers, *Ind. Engng Chem. Fundam.* **7**, 554–561 (1968).
2. G. A. Turner and L. Otten, Values of thermal (and other) parameters in packed beds, *Ind. Engng Chem. Process Des. Dev.* **12**, 417–424 (1973).
3. D. J. Gunn and J. F. C. De Souza, Heat transfer and axial dispersion in packed beds, *Chem. Engng Sci.* **29**, 1363–1371 (1974).
4. J. Shen, S. Kaguei and N. Wakao, Measurements of particle-to-gas heat transfer coefficients from one-shot thermal responses in packed beds, *Chem. Engng Sci.* **36**, 1283–1286 (1981).
5. W. H. McAdams, J. B. Pohlenz and R. C. St. John, Transfer of heat and mass between air and water in a packed tower, *Chem. Engng Prog.* **45**, 241–252 (1949).
6. H. S. Mickley, Design of forced draft air conditioning equipment, *Chem. Engng Prog.* **45**, 739–745 (1949).
7. H. Inazumi, Graphical determination of path curves on psychrometric chart in dehumidification and water cooling, *Kagaku Kogaku* (*Japan*) **14**, 148–153 (1950).
8. F. Yoshida and T. Tanaka, Air–water contact operations in a packed column, *Ind. Engng Chem.* **43**, 1468–1473 (1951).
9. S. L. Hensel, Jr. and R. E. Treybal, Air–water contact—adiabatic humidification of air with water in a packed tower, *Chem. Engng Prog.* **48**, 362–370 (1952).
10. S. Nori and T. Ishii, Humidification of air with warm water in countercurrent packed beds, *Chem. Engng Sci.* **37**, 487–490 (1982).
11. I. Yoshifuku, Sequential cell flowgraph representation for the cooling tower problem, *J. Chem. Engng Japan* **18**, 137–141 (1985).
12. M. A. Younis, M. A. Fahim and N. Wakao, Heat input-response in cooling tower—zeroth moments of temperature variations, *J. Chem. Engng Japan* **20**, 614–618 (1987).
13. N. Wakao and S. Kaguei, *Heat and Mass Transfer in Packed Beds*, pp. 12–15. Gordon & Breach, New York (1982).

ESTIMATION DE PARAMETRE POUR LE REFROIDISSEMENT DANS LE GARNISSAGE D'UNE TOUR, A PARTIR DE LA TECHNIQUE ENTREE-REPONSE THERMIQUE

Résumé—On propose une méthode pour prédire les variations des températures d'air, d'eau et celles de l'humidité de l'air dans un garnissage de tour de refroidissement à contre-courant, soumis à une perturbation thermique. Les mesures thermiques entrée-réponse sont faites en imposant des perturbations thermiques à l'eau entrante et à l'air entrant. Les coefficients de transfert thermique film d'air et film d'eau sont estimés en ajustant dans le domaine temporel les variations en sortie des températures et de l'humidité à celles calculées.

PARAMETER-ABSCHÄTZUNG FÜR DEN KÜHLTURMBETRIEB DURCH VERWENDUNG EINES STÖR-ANTWORT-VERFAHRENS

Zusammenfassung—Es wird ein Verfahren vorgestellt, mit dessen Hilfe es möglich ist, den Einfluß veränderter Eintrittstemperaturen auf die Luft- und Wassertemperaturen sowie die Luftfeuchtigkeit in einem Gegenstrom-Kühlturm zu bestimmen. Hierzu werden bei gezielter Störung des Eintrittszustandes Messungen der zeitlichen Veränderungen durchgeführt. Es werden die luft- und wasserseitigen Wärmeübergangskoeffizienten abgeschätzt, indem die gemessenen Temperatur/Feuchtigkeitsänderungen und die vorausberechneten angepaßt werden.

ОЦЕНКА РАБОЧИХ ПАРАМЕТРОВ ГРАДИРНИ С ПЛОТНОЙ НАСАДКОЙ МЕТОДОМ РЕАКЦИИ НА ТЕПЛОВУЮ НАГРУЗКУ

Аннотация—Предложен метод расчета изменений температуры воздуха и воды, а также влажности воздуха в градирне противоточного типа с плотной насадкой при наложении теплового возмущения. Тепловые измерения "возмущение—отклик" проводились путем создания температурных колебаний на входе воды и воздуха. Оценка коэффициентов теплопереноса от воздуха и воды к пленке производилась путем сопоставления измеренных значений температуры и влажности на выходе с рассчитанными в той же временной области.